A&A 481, 543–551 (2008)
DOI: 10.1051/0004-6361:20079073

Astronomy & Astrophysics

Atomic data from the IRON Project

LXV. Electron-impact excitation of Fe^{6+}

M. C. Witthoeft[1,2] and N. R. Badnell[1]

[1] Department of Physics, University of Strathclyde, Glasgow, G4 0NG, UK
[2] NASA Goddard Space Flight Center, Code 662, Greenbelt, MD 20771, USA
e-mail: witthoef@milkyway.gsfc.nasa.gov

Received 15 November 2007 / Accepted 16 January 2008

ABSTRACT

We present *R*-matrix results for the electron-impact excitation of Fe^{6+}. The intermediate-coupling frame transformation (ICFT) method has been used to obtain level-resolved collision strengths. We then calculate effective collision strengths assuming a Maxwellian distribution for the incident electron velocities. A large configuration interaction (CI) expansion of 1896 LS terms (4776 fine-structure levels) is used to obtain an accurate target. This is reduced to 89 close-coupling (CC) terms (189 levels) for the scattering calculation. To investigate the importance of CI, we also perform a second calculation with the same CC expansion but a smaller CI expansion. We discuss the difficulties of such a comparison and look at which transitions show the most sensitivity to the CI expansion. Our effective collision strengths are compared with a previous IRON Project report (Berrington et al. 2000, A&A, 142, 313) for transitions within the ground configuration and a recent distorted wave calculation (Zeng et al. 2005, MNRAS, 357, 440) for transitions to excited configurations. We find good agreement with the results of the previous *R*-matrix calculation and with the high-temperature distorted-wave results for most transitions, although there are some significant differences at lower temperatures in the latter case.

Key words. atomic data

1. Introduction

This work is carried out as part of the RmaX network[1] whose goal is to provide atomic data for transitions at X-ray wavelengths. As part of the IRON Project (Hummer et al. 1993), we are using *R*-matrix theory to calculate collision strengths for electron-impact excitation of Fe^{6+} to excited configurations. The advantage of the *R*-matrix approach is that the full resonance spectrum is calculated which is important at energies near the transition threshold.

Due to the complicated structure of Fe^{6+}, previous work on excitation is limited. Until recently, all previous calculations were confined to excitation within the ground configuration (Nussbaumer & Osterbrock 1970; Nussbaumer & Storey 1982; Berrington et al. 2000). The recent distorted-wave calculation of Zeng et al. (2005) is the first to provide effective collision strengths for transitions to excited levels. Their results are valid at higher temperatures where resonant enhancement is not important. The present calculations are performed using the *R*-matrix method which includes resonant enhancement. As Berrington et al. (2000) have already performed *R*-matrix calculations for excitation within the ground configuration of Fe^{6+}, our main focus in this work is on the excitation to excited configurations, namely the $3p^5\ 3d^3$ and $3p^6\ 3d\ 4l$ configurations.

The present calculations employ a large configuration-interaction (CI) expansion which is necessary to accurately represent the complex target. To help understand the effect of the CI expansion on the transitions to excited configurations, we have performed two *R*-matrix calculations. While each calculation has the same close-coupling (CC) expansion, the larger calculation, while only having 4 more configurations, has 2.5 times as many LS terms. The effect of these additional terms on the structure and collision strengths is examined.

For transitions within the ground configuration, our main comparison is with the *R*-matrix results of Berrington et al. (2000), who demonstrated the importance of resonant enhancement at low energies. For transitions to the excited configurations, we are comparing to the distorted wave calculations of Zeng et al. (2005), who used the Flexible Atomic Code (FAC) (Gu 2003).

The paper is organized as follows. In Sect. 2, we discuss the calculation method and compare our structure with previous calculations. The results are discussed in Sect. 3, where we cover convergence issues as well as compare to previous calculations. Finally, we summarize the important results of this work in Sect. 4.

2. Calculation

We have undertaken two complete scattering calculations using different CI expansions in order to examine the sensitivity of the resulting collision strengths. Previous calculations on Fe^{6+} by Nussbaumer & Storey (1982) and Berrington et al. (2000) have been used as a guide when choosing our CI expansions. The CI expansions of both our calculations are compared to those used by Berrington et al. (2000) and Zeng et al. (2005) in Table 1. The CI expansion of the first calculation consists of 738 LS terms and 1704 fine-structure levels while the larger calculation has 1896 terms and 4776 levels. While the inclusion of

[1] Web page: http://amdpp.phys.strath.ac.uk/UK_RmaX/

Table 1. Configuration interaction expansion used in present 36-configuration and 40-configuration calculations as well as those of Berrington et al. (2000) and Zeng et al. (2005).

Configuration	36-c.	40-c.	Berr.	Zeng
$3s^2\ 3p^6\ 3d^2$	•	•	•	•
$3s^2\ 3p^5\ 3d^3$	•	•	•	•
$3s^2\ 3p^6\ 3d\ 4l$	•	•	•	•
$3s^2\ 3p^6\ 3d\ 5l$	•	•		•
$3s\ 3p^6\ 3d^3$	•	•	•	•
$3s^2\ 3p^5\ 3d^2\ 4s$	•	•	•	•
$3s^2\ 3p^5\ 3d^2\ 4p$	•	•		
$3s^2\ 3p^5\ 3d^2\ 4d$	•	•		
$3s^2\ 3p^6\ 4l\ 4l'$	•	•	•	•
$3s^2\ 3p^4\ 3d^4$	•	•	•	•
$3s^2\ 3p^4\ 3d^3\ 4s$		•	•	
$3s^2\ 3p^4\ 3d^3\ 4p$		•	•	
$3s\ 3p^5\ 3d^4$		•		•
$3s^2\ 3p^3\ 3d^5$		•		•
$3s^2\ 3p^5\ 3d\ 4s^2$	•	•	•	
$3s^2\ 3p^6\ 4d\ 5l$	•	•		
$3p^6\ 3d^4$	•	•		
$3s^2\ 3p^6\ 5d^2$	•	•		
$3s^2\ 3p^6\ 5f^2$	•	•		
$3s^2\ 3p^6\ 5g^2$	•	•		

Table 2. Radial scaling factors used in AUTOSTRUCTURE to minimize the total energy of the *nl* orbital wave functions.

	36-config.	40-config.
λ_{1s}	1.4195	1.4239
λ_{2s}	1.1266	1.1281
λ_{2p}	1.0683	1.0695
λ_{3s}	1.1329	1.1287
λ_{3p}	1.1165	1.1129
λ_{3d}	1.1165	1.1205
λ_{4s}	1.1593	1.1415
λ_{4p}	1.1250	1.1126
λ_{4d}	1.1307	1.1314
λ_{4f}	1.2719	1.2738
λ_{5s}	1.1332	1.1339
λ_{5p}	1.1119	1.1134
λ_{5d}	1.1079	1.1077
λ_{5f}	1.0807	1.1093
λ_{5g}	1.1526	1.1657

the $3s^2\ 3p^4\ 3d^3\ 4l$ ($l = 0, 1$) configurations introduces 756 terms (2026 levels) into the CI expansion, they greatly improve the energies of the 3d 4s and 3d 4p levels. Ideally, one would like to include the $3s^2\ 3p^4\ 3d^3\ 4l$ ($l = 2, 3$) configurations as well, but the computation is too prohibitive at this time.

The wave functions used in the scattering calculation were obtained using AUTOSTRUCTURE (Badnell 1986). The target structure was calculated in the Thomas-Fermi approximation where the average of the LS term energies was optimized in a two-step procedure by adjusting the radial scaling parameters. In the first step, the average energy of all terms was optimized by allowing all scaling parameters (one for each orbital) to change. Then, the average energy of only the $3s^2\ 3p^6\ 3d\ 5l$ terms was optimized by changing the λ_{5l} scaling parameters. These scaling parameters are displayed in Table 2 for both calculations. The addition of the $3s^2\ 3p^4\ 3d^3\ 4s/4p$ improved the $3s^2\ 3p^6\ 3d\ 4s/4p$ energies by 0.24 Ry on average, to bring them into good agreement with observations. The level energies of the larger calculation are listed in Table 3 with those values compiled by NIST (Ralchencko et al. 2007).

Table 3. Energy levels in Rydbergs of the 40-configuration calculation compared to those listed in NIST (Ralchenko et al. 2007).

idx	Config.	Term	Present	NIST
1	$3p^6\ 3d^2$	$^3F_2$	0.0000	0.0
2	$3p^6\ 3d^2$	$^3F_3$	0.0117	0.0095820
3	$3p^6\ 3d^2$	$^3F_4$	0.0260	0.021246
4	$3p^6\ 3d^2$	$^1D_2$	0.1665	0.159248
5	$3p^6\ 3d^2$	$^3P_0$	0.1942	0.182621
6	$3p^6\ 3d^2$	$^3P_1$	0.1985	0.186173
7	$3p^6\ 3d^2$	$^3P_2$	0.2084	0.193905
8	$3p^6\ 3d^2$	$^1G_4$	0.2962	0.263605
9	$3p^6\ 3d^2$	$^1S_0$	0.6188	0.611262
10	$3p^6\ 3d\ 4s$	$^3D_1$	3.1095	3.138981
11	$3p^6\ 3d\ 4s$	$^3D_2$	3.1154	3.144133
12	$3p^6\ 3d\ 4s$	$^3D_3$	3.1280	3.155373
13	$3p^6\ 3d\ 4s$	$^1D_2$	3.1708	3.192466
14	$3p^5\ 3d^3$	$^5S_2$	3.5686	
15	$3p^5\ 3d^3$	$^5D_2$	3.6325	
16	$3p^5\ 3d^3$	$^5D_1$	3.6328	
17	$3p^5\ 3d^3$	$^5D_0$	3.6335	
18	$3p^5\ 3d^3$	$^5D_3$	3.6341	
19	$3p^5\ 3d^3$	$^5D_4$	3.6396	
20	$3p^5\ 3d^3$	$^5F_5$	3.7201	
21	$3p^5\ 3d^3$	$^5F_1$	3.7264	
22	$3p^5\ 3d^3$	$^5F_4$	3.7278	
23	$3p^5\ 3d^3$	$^5F_2$	3.7287	
24	$3p^5\ 3d^3$	$^5F_3$	3.7299	
25	$3p^6\ 3d\ 4p$	$^1D_2$	3.8392	3.876403
26	$3p^5\ 3d^3$	$^5G_6$	3.8394	
27	$3p^6\ 3d\ 4p$	$^3D_1$	3.8512	3.874057
28	$3p^6\ 3d\ 4p$	$^3D_2$	3.8608	3.898261
29	$3p^5\ 3d^3$	$^5G_5$	3.8630	
30	$3p^5\ 3d^3$	$^3F_2$	3.8649	
31	$3p^6\ 3d\ 4p$	$^3D_3$	3.8696	3.927093
32	$3p^6\ 3d\ 4p$	$^3F_3$	3.8802	3.922115
33	$3p^5\ 3d^3$	$^5G_4$	3.8805	
34	$3p^5\ 3d^3$	$^5G_3$	3.8962	
35	$3p^6\ 3d\ 4p$	$^3F_2$	3.8966	3.920393
36	$3p^6\ 3d\ 4p$	$^3F_4$	3.9045	3.953725
37	$3p^5\ 3d^3$	$^3D_2$	3.9281	
38	$3p^5\ 3d^3$	$^3F_3$	3.9334	
39	$3p^6\ 3d\ 4p$	$^3P_1$	3.9348	3.981801
40	$3p^5\ 3d^3$	$^5G_2$	3.9365	
41	$3p^6\ 3d\ 4p$	$^3P_0$	3.9410	3.982249
42	$3p^5\ 3d^3$	$^3D_3$	3.9512	
43	$3p^5\ 3d^3$	$^3F_4$	3.9535	
44	$3p^6\ 3d\ 4p$	$^3P_2$	3.9581	3.987322
45	$3p^5\ 3d^3$	$^3D_1$	3.9627	
46	$3p^6\ 3d\ 4p$	$^1F_3$	3.9910	4.007858
47	$3p^5\ 3d^3$	$^3P_0$	3.9948	
48	$3p^5\ 3d^3$	$^3P_2$	3.9953	
49	$3p^5\ 3d^3$	$^3P_1$	3.9962	
50	$3p^5\ 3d^3$	$^3G_3$	4.0026	
51	$3p^5\ 3d^3$	$^3G_4$	4.0068	
52	$3p^5\ 3d^3$	$^3G_5$	4.0097	
53	$3p^6\ 3d\ 4p$	$^1P_1$	4.0285	4.040986
54	$3p^5\ 3d^3$	$^3H_6$	4.1030	
55	$3p^5\ 3d^3$	$^1G_4$	4.1160	
56	$3p^5\ 3d^3$	$^3H_5$	4.1396	
57	$3p^5\ 3d^3$	$^3F_4$	4.1425	
58	$3p^5\ 3d^3$	$^3D_3$	4.1472	
59	$3p^5\ 3d^3$	$^3I_7$	4.1708	
60	$3p^5\ 3d^3$	$^3F_3$	4.1711	
61	$3p^5\ 3d^3$	$^5D_2$	4.1775	
62	$3p^5\ 3d^3$	$^1S_0$	4.1808	
63	$3p^5\ 3d^3$	$^5P_3$	4.1844	
64	$3p^5\ 3d^3$	$^3H_4$	4.1919	

Table 3. continued.

idx	Config.	Term	Present	NIST
65	$3p^5\ 3d^3$	$^5D_1$	4.1935	
66	$3p^5\ 3d^3$	$^3D_2$	4.1971	
67	$3p^5\ 3d^3$	$^3I_6$	4.1995	
68	$3p^5\ 3d^3$	$^3F_2$	4.2007	
69	$3p^5\ 3d^3$	$^5D_4$	4.2063	
70	$3p^5\ 3d^3$	$^3D_1$	4.2153	
71	$3p^5\ 3d^3$	$^5D_0$	4.2196	
72	$3p^5\ 3d^3$	$^5D_3$	4.2281	
73	$3p^5\ 3d^3$	$^3I_5$	4.2433	
74	$3p^5\ 3d^3$	$^5P_1$	4.2477	
75	$3p^5\ 3d^3$	$^5P_2$	4.2493	
76	$3p^5\ 3d^3$	$^3G_3$	4.2671	
77	$3p^5\ 3d^3$	$^3P_1$	4.2835	
78	$3p^5\ 3d^3$	$^3P_2$	4.2847	
79	$3p^5\ 3d^3$	$^3P_0$	4.2908	
80	$3p^5\ 3d^3$	$^3G_4$	4.3028	
81	$3p^5\ 3d^3$	$^3G_5$	4.3122	
82	$3p^5\ 3d^3$	$^1F_3$	4.3173	
83	$3p^5\ 3d^3$	$^1D_2$	4.3174	
84	$3p^5\ 3d^3$	$^3S_1$	4.3322	
85	$3p^5\ 3d^3$	$^3D_1$	4.3525	
86	$3p^5\ 3d^3$	$^1I_6$	4.3559	
87	$3p^5\ 3d^3$	$^3D_2$	4.3631	
88	$3p^5\ 3d^3$	$^3D_3$	4.3816	
89	$3p^5\ 3d^3$	$^1P_1$	4.3876	
90	$3p^5\ 3d^3$	$^3F_4$	4.3950	
91	$3p^5\ 3d^3$	$^3H_4$	4.4067	
92	$3p^5\ 3d^3$	$^3H_5$	4.4075	
93	$3p^5\ 3d^3$	$^1H_5$	4.4186	4.22859
94	$3p^5\ 3d^3$	$^3F_3$	4.4361	
95	$3p^5\ 3d^3$	$^3F_2$	4.4453	
96	$3p^5\ 3d^3$	$^3H_6$	4.4508	
97	$3p^5\ 3d^3$	$^3G_5$	4.4787	4.30627
98	$3p^5\ 3d^3$	$^3G_4$	4.4836	4.30941
99	$3p^5\ 3d^3$	$^3P_0$	4.4964	
100	$3p^5\ 3d^3$	$^1D_2$	4.4969	
101	$3p^5\ 3d^3$	$^3G_3$	4.5110	4.38716
102	$3p^5\ 3d^3$	$^3P_1$	4.5112	
103	$3p^5\ 3d^3$	$^3P_2$	4.5453	
104	$3p^5\ 3d^3$	$^1G_4$	4.6474	4.52402
105	$3p^5\ 3d^3$	$^3F_4$	4.7687	
106	$3p^5\ 3d^3$	$^3G_3$	4.7803	4.64825
107	$3p^5\ 3d^3$	$^3F_3$	4.7995	
108	$3p^5\ 3d^3$	$^3G_4$	4.8084	4.64890
109	$3p^5\ 3d^3$	$^3F_2$	4.8222	
110	$3p^5\ 3d^3$	$^3G_5$	4.8288	4.68512
111	$3p^5\ 3d^3$	$^1F_3$	4.9860	
112	$3p^5\ 3d^3$	$^3D_3$	5.0379	
113	$3p^5\ 3d^3$	$^3D_2$	5.0397	
114	$3p^5\ 3d^3$	$^3D_1$	5.0485	
115	$3p^5\ 3d^3$	$^1D_2$	5.0556	4.90526
116	$3p^5\ 3d^3$	$^1H_5$	5.0724	
117	$3p^5\ 3d^3$	$^3D_1$	5.1802	
118	$3p^5\ 3d^3$	$^3D_2$	5.1871	4.99624
119	$3p^5\ 3d^3$	$^1F_3$	5.1948	
120	$3p^5\ 3d^3$	$^3D_3$	5.2365	5.02626
121	$3p^5\ 3d^3$	$^1D_2$	5.2426	5.04131
122	$3p^6\ 3d\ 4d$	$^1F_3$	5.2728	5.07049
123	$3p^6\ 3d\ 4d$	$^3D_1$	5.2878	
124	$3p^6\ 3d\ 4d$	$^3D_2$	5.2947	
125	$3p^6\ 3d\ 4d$	$^3D_3$	5.3024	
126	$3p^5\ 3d^3$	$^3P_0$	5.3070	
127	$3p^6\ 3d\ 4d$	$^3G_3$	5.3095	
128	$3p^6\ 3d\ 4d$	$^1P_1$	5.3135	

Table 3. continued.

idx	Config.	Term	Present	NIST
129	$3p^6\ 3d\ 4d$	$^3G_4$	5.3172	
130	$3p^5\ 3d^3$	$^3P_1$	5.3195	5.11497
131	$3p^5\ 3d^3$	$^3F_2$	5.3198	5.14342
132	$3p^6\ 3d\ 4d$	$^3G_5$	5.3284	
133	$3p^5\ 3d^3$	$^3F_3$	5.3363	5.16010
134	$3p^5\ 3d^3$	$^3P_2$	5.3545	5.15116
135	$3p^5\ 3d^3$	$^3F_4$	5.3556	5.17707
136	$3p^6\ 3d\ 4d$	$^3S_1$	5.3636	
137	$3p^6\ 3d\ 4d$	$^3F_2$	5.3960	
138	$3p^6\ 3d\ 4d$	$^3F_3$	5.4039	
139	$3p^6\ 3d\ 4d$	$^3F_4$	5.4126	
140	$3p^6\ 3d\ 4d$	$^1D_2$	5.4684	
141	$3p^6\ 3d\ 4d$	$^3P_0$	5.4770	
142	$3p^6\ 3d\ 4d$	$^3P_1$	5.4804	
143	$3p^6\ 3d\ 4d$	$^3P_2$	5.4874	
144	$3p^6\ 3d\ 4d$	$^1G_4$	5.5127	
145	$3p^6\ 3d\ 4d$	$^1S_0$	5.6444	
146	$3p^5\ 3d^3$	$^1P_1$	5.6463	5.45519
147	$3p^5\ 3d^3$	$^3D_2$	5.6871	5.50184
148	$3p^5\ 3d^3$	$^3D_3$	5.6887	5.49876
149	$3p^5\ 3d^3$	$^3D_1$	5.6907	5.50651
150	$3p^5\ 3d^3$	$^1G_4$	5.6995	5.51762
151	$3p^5\ 3d^3$	$^3S_1$	5.8333	5.68356
152	$3p^5\ 3d^3$	$^1P_1$	5.9025	5.74356
153	$3p^5\ 3d^3$	$^1F_3$	5.9644	
154	$3p^6\ 3d\ 5s$	$^3D_1$	6.1637	
155	$3p^6\ 3d\ 5s$	$^3D_2$	6.1675	
156	$3p^6\ 3d\ 5s$	$^3D_3$	6.1818	
157	$3p^6\ 3d\ 5s$	$^1D_2$	6.1938	
158	$3p^6\ 3d\ 4f$	$^3H_4$	6.2307	
159	$3p^6\ 3d\ 4f$	$^3H_5$	6.2382	
160	$3p^6\ 3d\ 4f$	$^3H_6$	6.2477	
161	$3p^6\ 3d\ 4f$	$^1G_4$	6.2716	6.01361
162	$3p^6\ 3d\ 4f$	$^3F_2$	6.2724	6.01450
163	$3p^6\ 3d\ 4f$	$^3F_3$	6.2763	6.01762
164	$3p^6\ 3d\ 4f$	$^3F_4$	6.2843	6.02502
165	$3p^6\ 3d\ 4f$	$^3G_3$	6.3157	6.04258
166	$3p^6\ 3d\ 4f$	$^1D_2$	6.3203	6.04964
167	$3p^6\ 3d\ 4f$	$^3G_4$	6.3240	6.05036
168	$3p^6\ 3d\ 4f$	$^3G_5$	6.3303	6.05521
169	$3p^6\ 3d\ 4f$	$^1F_3$	6.3412	6.06373
170	$3p^6\ 3d\ 4f$	$^3D_1$	6.3440	6.06751
171	$3p^6\ 3d\ 4f$	$^3D_2$	6.3448	6.06834
172	$3p^6\ 3d\ 4f$	$^3D_3$	6.3537	6.07497
173	$3p^6\ 3d\ 4f$	$^3P_2$	6.3628	6.08634
174	$3p^6\ 3d\ 4f$	$^3P_1$	6.3655	6.08957
175	$3p^6\ 3d\ 4f$	$^3P_0$	6.3674	6.09172
176	$3p^6\ 3d\ 4f$	$^1H_5$	6.3997	6.10529
177	$3p^6\ 3d\ 4f$	$^1P_1$	6.4268	6.13119
178	$3p^6\ 3d\ 5p$	$^1D_2$	6.4720	
179	$3p^6\ 3d\ 5p$	$^3D_1$	6.4756	
180	$3p^6\ 3d\ 5p$	$^3D_2$	6.4843	
181	$3p^6\ 3d\ 5p$	$^3F_2$	6.4910	
182	$3p^6\ 3d\ 5p$	$^3D_3$	6.4936	
183	$3p^6\ 3d\ 5p$	$^3F_3$	6.4955	
184	$3p^6\ 3d\ 5p$	$^3F_4$	6.5098	
185	$3p^6\ 3d\ 5p$	$^3P_0$	6.5113	
186	$3p^6\ 3d\ 5p$	$^3P_1$	6.5120	
187	$3p^6\ 3d\ 5p$	$^3P_2$	6.5233	
188	$3p^6\ 3d\ 5p$	$^1F_3$	6.5371	
189	$3p^6\ 3d\ 5p$	$^1P_1$	6.5486	

Table 4. Einstein A-coefficients (in s^{-1}) for transitions between the ground configuration of the present 40-configuration calculation compared to Nussbaumer & Storey (1982) (N&S) and Berrington et al. (2000) (Berr.). The superscript denotes the power of 10.

i	j	Present	N&S	Berr.
1	2	5.37^{-2}	2.98^{-2}	3.25^{-2}
1	3	3.75^{-9}	1.34^{-9}	1.67^{-9}
1	4	4.81^{-1}	3.60^{-1}	3.72^{-1}
1	5	1.34^{-1}	9.37^{-2}	1.35^{-1}
1	6	5.09^{-2}	3.55^{-2}	5.02^{-2}
1	7	2.25^{-2}	1.93^{-2}	1.50^{-2}
1	8	1.31^{-3}	5.55^{-4}	9.59^{-4}
1	9	2.12^{-1}	1.67^{-1}	1.81^{-1}
2	3	7.91^{-2}	4.24^{-2}	4.66^{-2}
2	4	7.65^{-1}	5.77^{-1}	6.03^{-1}
2	6	7.29^{-2}	5.25^{-2}	7.62^{-2}
2	7	9.48^{-2}	7.69^{-2}	6.97^{-2}
2	8	4.30^{-1}	3.14^{-1}	3.43^{-1}
3	4	1.61^{-3}	1.55^{-3}	1.39^{-3}
3	7	6.91^{-2}	4.96^{-2}	7.35^{-2}
3	8	6.42^{-1}	4.54^{-1}	5.03^{-1}
4	5	4.38^{-7}	2.07^{-7}	4.72^{-7}
4	6	6.34^{-2}	4.37^{-2}	5.72^{-2}
4	7	2.41^{-1}	1.56^{-1}	1.82^{-1}
4	8	4.08^{-3}	1.23^{-3}	4.14^{-3}
4	9	2.36^{+1}	2.17^{+1}	2.67^{+1}
5	6	1.85^{-3}	1.06^{-3}	1.15^{-3}
5	7	4.55^{-8}	1.39^{-8}	1.39^{-8}
6	7	1.63^{-2}	7.62^{-3}	7.43^{-3}
6	9	8.77	6.93	6.88
7	8	5.49^{-5}	1.74^{-5}	4.54^{-5}
7	9	1.25	1.39	1.11

In Fe^{6+}, the $3s^2\ 3p^6\ 3d\ 4l$ levels overlap strongly with the the $3s^2\ 3p^5\ 3d^3$ levels. While this does not influence the 3d 4s or 3d 4d levels much, there is strong mixing of the $2p^5\ 3d^3$ levels with the 3d 4p and 3d 4f levels. This mixing makes it difficult to perform comparisons with other calculations which use different CI-expansions (thereby changing the mixing). This difficulty is very pronounced between the two present calculations. To uniquely identify a level only the total angular momentum (J), the parity, and the energy order are needed. In this case, however, we have found that using the configuration as a good quantum number yields better results. Still, the mapping is not perfect and some levels in one calculation do not have a strict analog in another calculation. This will be discussed in more detail in Sect. 3.2.

In Table 4, we show Einstein A-coefficients for transitions between the ground configuration compared with Nussbaumer & Storey (1982) and Berrington et al. (2000). The A-coefficients for both present calculations agree well with each other, so only the values from the larger calculation are shown in the table. For many of the transitions, our A-coefficients are larger than the two previous calculations which, for the most part, agree well with each other. There are several transitions (for example, 4−5, 4−8, 7−8), where the present A-coefficients are in much better agreement with Berrington et al. than Nussbaumer & Storey. Note: the A-coefficients listed for Berrington et al. (2000) for the 1−4, 1−7, and 4−7 transitions have been corrected from the published text (private communication, Berrington).

The A-coefficients of both present calculations for transitions to the $3s^2\ 3p^6\ 3d\ 4s$ levels are listed in Table 5 along with those from Warner & Kirkpatrick (1969). Here, we see that the 40-configuration A-coefficients are in much better agreement

Table 5. A-coefficients (in s^{-1}) for transitions to the $3s^2\ 3p^6\ 3d\ 4s$ levels from the ground configuration. Values from both present calculations are compared to those in Warner & Kirkpatrick (1969) (W&K). The superscript denotes the power of 10.

i	j	36-config.	40-config.	W&K
1	10	1.96^{+5}	1.36^{+5}	1.23^{+5}
1	11	8.56^{+4}	5.95^{+4}	5.36^{+4}
1	12	5.93^{+3}	4.14^{+3}	3.80^{+3}
1	13	2.79^{+2}	2.41^{+2}	3.23^{+2}
2	10	9.81^{+4}	6.80^{+4}	6.08^{+4}
2	11	1.44^{+5}	9.97^{+4}	8.96^{+4}
2	12	6.36^{+4}	4.43^{+4}	4.02^{+4}
2	13	3.79^{+3}	2.91^{+3}	2.65^{+3}
3	11	6.23^{+4}	4.31^{+4}	3.84^{+4}
3	12	2.25^{+5}	1.57^{+5}	1.41^{+5}
3	13	6.48^{+2}	5.12^{+2}	4.58^{+2}
4	10	4.57^{+3}	3.15^{+3}	2.36^{+3}
4	11	1.19^{+4}	8.62^{+3}	7.58^{+3}
4	12	4.99^{+3}	3.47^{+3}	3.02^{+3}
4	13	1.70^{+5}	1.17^{+5}	9.83^{+4}
5	11	3.16^{+4}	2.16^{+4}	1.96^{+4}
5	13	5.26^{+2}	4.00^{+2}	3.60^{+2}
6	10	7.18^{+4}	4.91^{+4}	4.42^{+4}
6	11	7.80^{+3}	5.33^{+3}	4.82^{+3}
6	12	3.22^{+4}	2.22^{+4}	2.01^{+4}
6	13	2.07^{+2}	1.57^{+2}	1.44^{+2}
7	10	2.05^{+4}	1.40^{+4}	1.28^{+4}
7	11	4.48^{+4}	3.03^{+4}	2.76^{+4}
7	12	5.94^{+4}	4.07^{+4}	3.71^{+4}
7	13	2.17^{+4}	1.53^{+4}	1.26^{+4}
8	11	5.70^{+3}	4.20^{+3}	3.68^{+3}
8	12	1.36^{+2}	9.10^{+1}	5.61^{+1}
8	13	2.68^{+5}	1.81^{+5}	1.67^{+5}
9	11	2.03^{+2}	1.55^{+2}	1.58^{+2}
9	13	1.70^{+4}	1.14^{+4}	1.03^{+4}

(10%) with Warner & Kirkpatrick than the 36-configuration values which, on average, are 60% higher. A-coefficients for transitions to $3s^2\ 3p^6\ 3d\ 4p/4f$ and $3s^2\ 3p^5\ 3d^3$ levels will be examined in coincidence with the effective collision strengths in the Sect. 3.4. Here, we will just mention that we find overall very good agreement with both Zeng et al. (2005) and Quinet & Hansen (1996).

The scattering calculations were performed using R-matrix theory (Wigner & Eisenbud 1947; Burke & Berrington 1993) where the the intermediate-coupling frame transformation method (ICFT) of Griffin et al. (1998) was used to simplify the inner region calculation. The details of the calculations follow closely to previous work on iron ions (cf. Witthoeft et al. 2007). The large CI-expansion was cut back to a small close-coupling expansion of 89 terms (189 levels) in both present calculations. This step can be done early in the ICFT calculation, greatly simplifying the rest of the calculation. The configurations retained in the close-coupling expansion are $3s^2\ 3p^6\ 3d^2$, $3s^2\ 3p^5\ 3d^3$, $3s^2\ 3p^6\ 3d\ 4l$, and $3s^2\ 3p^6\ 3d\ 5l$ ($l = 0, 1$).

Exchange effects were included in the inner region calculation up to $J = 14$ which was extended to $J = 40$ with a non-exchange calculation before being topped up to infinite J using the Burgess sum rule (Burgess 1974) for dipole transitions and a geometric series for the non-dipole transitions (Badnell & Griffin 2001). For the resonance region in the outer region calculation, we used an energy mesh of $10^{-5}z^2$ Ry for the 36-configuration calculation and $5 \times 10^{-6}z^2$ Ry for the 40-configuration calculation, where $z = 6$ is the residual charge of the ion. An energy

mesh of $10^{-4}z^2$ Ry was used beyond the resonance region of the exchange calculation and a mesh of $10^{-3}z^2$ Ry was used for the entire non-exchange calculation. The calculations were carried out up to an impact energy of 2.5 times the ionization threshold. The collision strengths for each transition were then convoluted with a Maxwellian distribution to obtain effective collision strengths. For high temperatures, we interpolated the R-matrix collision strengths to an infinite energy point calculated using AUTOSTRUCTURE (see Whiteford et al. 2001).

3. Results

3.1. Convergence of resonant enhancement

In order to check the convergence of the effective collision strengths, two different energy meshes (10^{-5} and 5×10^{-6} z^2 Ry) were used in the 40-configuration calculation. The differences from the two energy resolutions are most apparent at the lowest tabulated temperature where we find that only 1% of all transitions have an effective collision strength differing by greater than 10%. When examining only transitions from the ground configuration, less than a half percent (or 6 transitions) disagree by greater than 10%; only two of these disagree by more than 20%. The agreement between the calculations using the two energy meshes rapidly improves with increasing temperature. From this result, we consider this collection of effective collision strengths to be converged with respect to resonance resolution.

3.2. Sensitivity with CI expansion

A comparison between the 36- and 40-configuration results is complicated by the difficulty in matching the levels between the two calculations. A normal mapping of the levels is done by considering only the total angular momentum (J), the parity, and the energy order of the level to be good quantum numbers. However, for this case, we achieve better results if we also consider the configuration as a good quantum number. Even after this consideration, though, the matching is not perfect and we need to identify which levels do not actually correspond to one another. We do this by considering the term coupling coefficients from the structure calculation. The overlap of a level from two different calculations can be determined in the following way:

$$\mathrm{overlap}(l, l') = \sum_t |f(l,t)\bar{f}(l',t')| \quad (1)$$

where f and $\bar{f}$ are the term coupling coefficients from each calculation and l and t designate the level and term indices respectively. The term indices, t', in the second coefficient must be mapped uniquely to the term indices appearing in the first coefficient. Here, the term mapping has been done by considering the configuration, term label, and energy order to be good quantum numbers. Since the terms from each calculation are not equivalent, these overlap numbers can only serve to indicate which level mappings are poor; there is no significance in the actual value. Levels from the two calculations which correspond well to each other will have an overlap near to unity. To see the importance of identifying poorly matched levels, we show in Fig. 1 the ratio of effective collision strengths for transitions from the ground level at $T = 9.8 \times 10^7$ K between the 36- and 40-configuration calculations as a function of the effective collision strength of the larger calculation. We have circled transitions to levels which have an overlap less than 0.9. We see that most of the transitions which show the largest disagreement also have a poorly matched final level. Due to the different configuration expansions of the structure, some levels from the two calculations simply cannot be matched well to each other. Primarily, it is mixing of the 4p/4f levels with the $3d^3$ levels that show the smallest overlaps between the two calculations; these levels would be better matched by removing the configuration as a good quantum number. However, since comparisons with other calculations will be made using the configuration as a good quantum number, we will not adjust the level mapping for the comparison between the present calculations and, instead, we will discount levels with an overlap less than 0.9.

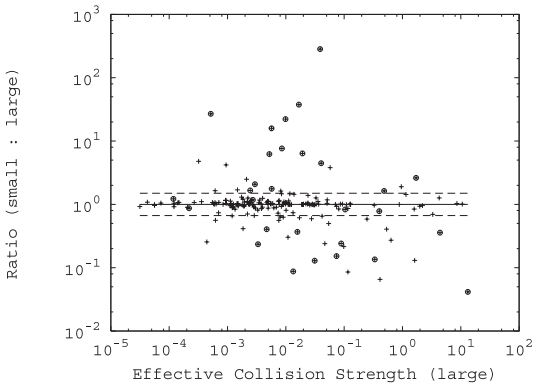

Fig. 1. Ratio of effective collision strengths between the present 36- and 40-configuration calculations at $T = 9.8 \times 10^7$ K. Only transitions from the ground level are shown. Circled points correspond to transitions where the final level is poorly matched (overlap less than 0.9) between the two calculations.

Once transitions with poorly matched levels have been removed, a meaningful comparison between the 36- and 40-configuration calculations can be performed. For transitions within the ground configuration, we find excellent agreement between the present calculations. Over the entire tabulated temperature range (9.8×10^3–9.8×10^7 K) the effective collision strengths for these transitions agree within 10%.

We see more differences for transitions to the excited configurations. In Figs. 2 and 3, we show transitions to the $4l$ levels at our lowest and highest tabulated temperatures. At the low temperature, we see that the larger calculation yields considerably larger effective collision strengths for transitions to the 4s and 4p levels. At the high temperature, however, the calculations are in excellent agreement apart from a couple of the 4p transitions. This behavior indicates that the larger calculation has more resonant enhancement for these transitions. The reason for the large disagreement at high temperatures for some of the 4p transitions is most likely due to remaining differences in mixing of the 4p and $3d^3$ levels between the two calculations. For transitions to the 4d levels, it appears that it is the smaller calculation that has more resonant enhancement. Finally, for the 4f transitions, we see generally good agreement between the two calculations at all temperatures. There is more scatter for these transitions at low temperatures due to differences in resonance structure but, on average, the two calculations yield similar results. There is also mixing between the 4f and $3d^3$ levels which shows up at high temperatures for some transitions showing large disagreement (see Fig. 3). Since the addition of the $3s^2$ $3p^4$ $3d^3$ 4s/4p levels significantly improved the 4s and 4p level energies in the larger calculation, we expect that the differences in the low temperature effective collision strengths for the $4l$ transitions are due to these configurations. Undoubtedly, the inclusion of the $3s^2$ $3p^4$ $3d^3$ 4d/4f levels would further affect these transitions, but that CI expansion is too large to handle at present. For transitions

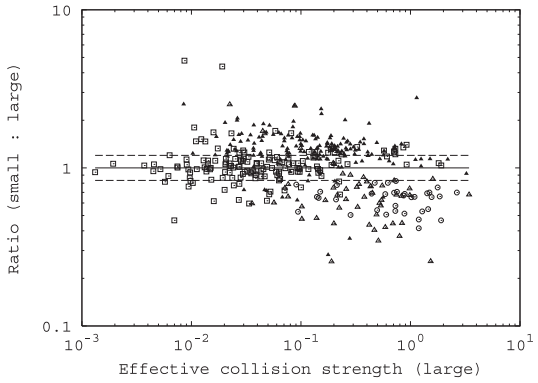

Fig. 2. Ratio of effective collision strengths between the present 36- and 40-configuration calculations at $T = 9.8 \times 10^3$ K for transitions from the ground configuration to the 4*l* configurations: 4s (circles), 4p (open triangles), 4d (filled triangles), 4f (squares).

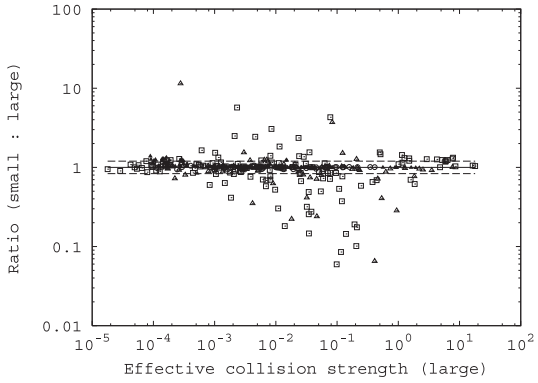

Fig. 3. Same as Fig. 2 but with $T = 9.8 \times 10^7$ K.

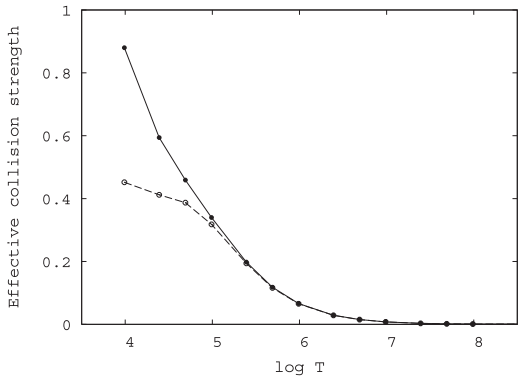

Fig. 4. Effective collision strength for the 3−10 transition from the 40-configuration calculation (filled circles) and the 36-configuration calculation (open circles).

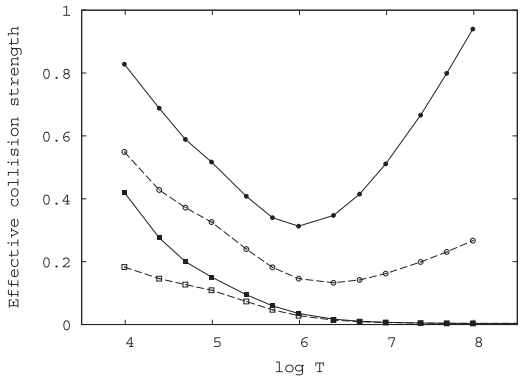

Fig. 5. Effective collision strength for the 2−31 (circles) and 3−27 (squares) transitions from the 40-configuration calculation (filled symbols) and the 36-configuration calculation (open symbols).

to the $2p^5\ 3d^3$ levels, we see similar results as for transitions to the 3d 4f levels.

To further demonstrate the conclusions reached above, we show the effective collision strengths for a couple 4*l* transitions. In Fig. 4, is the effective collision strength for the 3−10 transition from both present calculations. For this 4s transitions, we see that the two calculations agree very well for moderate to high temperatures, but that the larger calculation has considerably more resonant enhancement at low temperatures. This additional resonant enhancement is due to resonances near threshold. In Fig. 5, we compare the present results for two transitions to 4p levels (note that both levels have considerable mixing with $2p^5\ 3d^3$ levels). While the larger calculation shows more resonant enhancement at low temperatures for both transitions, there is a large difference in the agreement at high temperatures. For the transition showing good agreement at high temperatures, the overlap of the final level between both calculations is 0.99, while the overlap for the final level of the other transition is 0.96. This indicates that differences in the mixing between the two calculations is changing the high-temperature behavior of the latter transition. The high-temperature behavior of the 2−31 transition is determined by the oscillator strength, where there is a factor of four difference between the 40- and 36-configuration calculations.

Taking a closer look at the mixing for level 31, we find that, in the smaller calculation, this level is strongly mixed with several $3d^3\ ^3D_3$ levels. While the larger calculation shows less mixing overall, it is most strongly mixed with the $4p\ ^3F_3$ level. Whereas the collision strengths for transitions from level 2 to the $3d^3\ ^3D_3$ levels are weak at high temperatures, the transition to the $4p\ ^3F_3$ is very strong. Because of the change in level mixing, the large increase we see in the effective collision strength for the 2−31 transition when going from the 36- to 40-configuration calculation is matched by a large decrease in the effective collision strength forthe transition to the $4p\ ^3F_3$ level (labeled 32 in the 40-configuration calculation).

For the rest of the paper, the present results refer to the 40-configuration calculation.

3.3. Transitions among the ground configuration

For transitions between the levels in the ground configuration, the present results agree well with the results of Berrington et al. (2000). Over the entire temperature range, more than two-thirds of the transitions agree to better than 10% and, at most, 6 transitions disagree by more than 20% at any temperature. The best agreement between the two calculations is for temperatures in the middle of the tabulated range of Berrington et al., where only 2 transitions disagree by more than 20% (8−9 and 4−8). At the low-end of the temperature range ($T = 2 \times 10^4$ K), differences in resonant enhancement are the cause for the disagreement. In Fig. 6, we show the ratio of the effective collision strengths from Berrington et al. to the present results at a temperature of $T = 2 \times 10^4$ K. The transitions which disagree by more than 20% are labeled, except for the 8−9 transition which is off the scale of the plot with a ratio near to 2.5. We show the effective collision strengths as a function of temperature for the 1−7 and 8−9 transitions in Fig. 7. While the effective

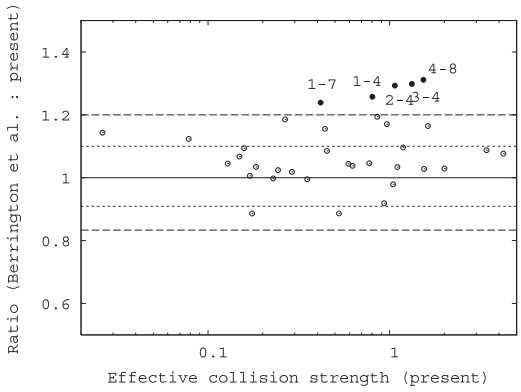

Fig. 6. Ratio of the effective collision strengths of transitions between the levels of the ground configuration from Berrington et al. (2000) to the present, 40-configuration calculation at a temperature of 2×10^4 K. The filled symbols mark transitions where the agreement is worse than 20%.

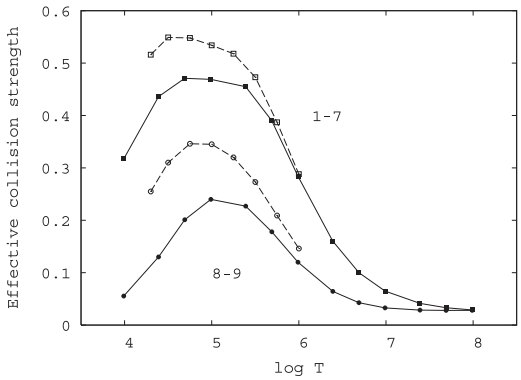

Fig. 7. Effective collision strengths for the 1−7 (squares) and 8−9 (circles) transitions. Solid curves with filled symbols are the present, 40-configuration results and the dashed curves with open symbols are from Berrington et al. (2000).

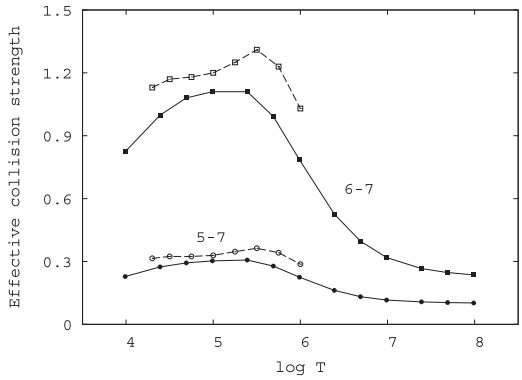

Fig. 8. Effective collision strengths for the 6−7 (squares) and 5−7 (circles) transitions. Solid curves with filled symbols are the present, 40-configuration results and the dashed curves with open symbols are from Berrington et al. (2000).

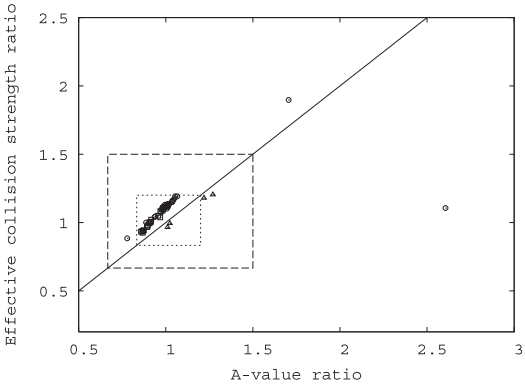

Fig. 9. Comparison of results from Zeng et al. (2005) to the present 40-configuration results at $T = 5.80 \times 10^6$ K. Points represent transitions from the ground configuration to levels in the $3d^3$ (circles), 4p (triangles), and 4f (squares) configurations. On the x-axis is shown the ratio of the A-coefficients from the Zeng et al. calculation to the present calculation; on the y-axis is the analagous ratio of the effective collision strengths. The dotted and dashed boxes correspond to agreement within 20% and 50%. The solid line marks where the ratios agree.

collision strengths are coming into agreement at high temperatures, Berrington et al. gives appreciably larger values at the low temperatures. These differences are most likely due to differences in the target structure between the two calculations. Although Berrington et al. used an energy mesh 4 times coarser than the present calculation (Berrington, private communication), it is unlikely to be the primary reason of the large differences we see with Berrington et al. for these transitions. We base this conclusion on the good convergence we see with our own calcluation with respect to energy mesh.

At higher temperatures, the transitions which disagreed at low-temperatures now agree with the exception of the 8−9 transition. However, transitions among levels 5, 6, and 7 now disagree by more than 20%. We show the effective collision strengths for two of these transitions in Fig. 8. For these transitions, it appears that resonances are playing a large role at high temperatures. Had Berrington et al. continued their calculation to higher temperatures, we expect that their results would come into agreement with ours.

3.4. Transitions to excited configurations

Since both the present calculation and that of Zeng et al. (2005) have such large configuration expansions, we expect to see good agreement between the two results for high impact energies. The results of Zeng et al. do not include resonant enhancement, therefore they only tabulate their results down to a temperature of 1.16×10^5 K. At this temperature resonance effects are just starting to become important, so we expect to see more differences here.

In Fig. 9, we show a comparison between the effective collision strengths and A-coefficients of the Zeng et al. calculation and the present calculation at the highest tabulated temperature of Zeng et al. (5.80×10^6 K). At this temperature, there is little resonant enhancement of the effective collision strength and we expect to see the best agreement. Overall, this is exactly what we see. For the vast majority of the transitions, the agreement of both the A-coefficients and the effective collision strengths are within 20%. Furthermore, we can plainly see the strong dependence of the effective collision strength on the magnitude of the A-coefficient since, for transitions with a larger disagreement in the A-coefficient, we see a corresponding difference in the effective collision strength. The solid line shows where the ratios agree and we find that the effective collision strengths of Zeng et al. are systematically larger than the present calculation with respect to this line for transitions to the $3d^3$ and 4f configurations. The present results, however, are slightly larger for the few 4p transitions shown. There are two transitions where the present results disagree strongly with Zeng et al.; the 1−107 transition with an A-coefficient ratio of 1.7 and the 2−148 transition

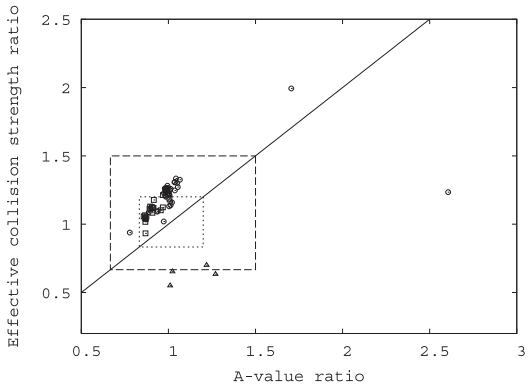

Fig. 10. Same as Fig. 10 except with $T = 1.16 \times 10^5$ K.

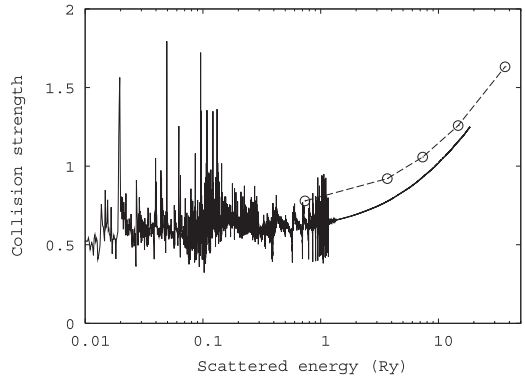

Fig. 11. Collision strength for the 5−117 transition from the present, 40-configuration calculation (solid curve) and the (a) calculation of Zeng et al. (2005) (dashed curve with circles).

which has an A-coefficient ratio of 2.6. Only the 1−107 transition shows disagreement of the effective collision strength by more than 20%. The reason for these disparate points may be due to mixing, but we can not say for sure. In the Zeng et al. text, these transitions are labeled as 1−107 and 2−147, respectively.

In Fig. 10, we show a similar plot as Fig. 9 but for the lowest tabulated temperature of Zeng et al. (1.16×10^5 K). Because of resonant enhancement, we expect to see the effective collision strength ratio decrease, but we find that it has increased for nearly all of the $3d^3$ and 4f transitions. Only transitions to the 4p levels show the behavior which we expect, that is, evidence of resonant enhancement. For transitions to the $3d^3$ levels, resonant enhancement is a small to moderate effect (10−30%) and, although the A-coefficients are in agreement for these transitions, the Zeng et al. results have a consistently larger background collision strength at all temperatures (see Fig. 11). For the transitions to the 4f levels, we see almost no resonant enhancement of the present results and the effective collision strengths are in very good agreement with the Zeng et al. results despite the smaller A-coefficients. For the 4p transitions, the background collision strengths are in good agreement, but there is significant resonant enhancement in the present calculations which decreases the ratio at low temperatures (see Fig. 12).

In Zeng et al. (2005), two calculations were performed using different amounts of CI. They reported that the effective collision strengths from the larger calculation were systematically smaller than those from the small-CI calculation. With the exception of the 3d 4p transitions, we are seeing a similar trend here, as our present calculation has a larger CI than that used by Zeng et al. We have also shown this trend in the comparison between our

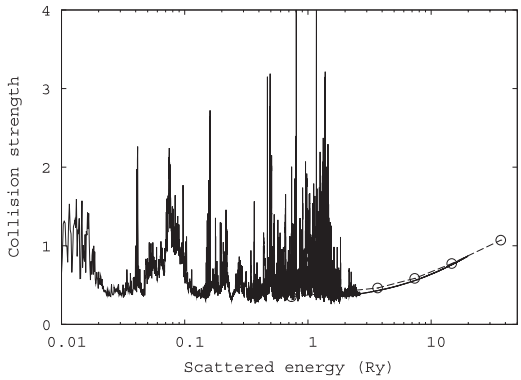

Fig. 12. Collision strength for the 1−27 transition from the present, 40-configuration calculation (solid curve) and the (a) calculation of Zeng et al. (2005) (dashed curve with circles).

own 36- and 40-configuration calculations in Sect. 3.2. Again, with the exception of the transitions to the 3d 4p levels, the resonant enhancement of the present calculation at the lowest tabulated temperature of Zeng et al. was not sufficient to overcome this systematic lowering of the effective collision strength. We do see, however, more variability in the agreement between the present calculation and Zeng et al. which is due to resonant enhancement in the present results.

At low temperatures, the impact of resonant enhancement on the effective collision strength is highly dependent on the type of transition. We find that resonant enhancement is largest for transitions to the 4s levels, where the effective collision strength is typically enhanced by a factor of 10−15 at a temperature of 10^5 K. An example of this can be seen for the 4s transition shown in Fig. 4 where the background collision strength for this transition is approximately 0.01. The strongest transitions to the 4p levels are approximately doubled, although some can increase by an order of magnitude. For the strongest transitions to the 4d levels, we find an increase of around 30−50% while transitions to the 4f levels are hardly affected. Resonant enhancement can play a large role for the weaker transitions to the $3d^3$ levels, but little enhancement is seen for the strongest transitions.

4. Summary

We have calculated collision strengths and effective collision strengths for electron-impact excitation of Fe^{6+}. We studied the sensitivity of the collision strengths by performing two calculations with different amounts of CI and found that the inclusion of the $3s^2\ 3p^4\ 3d^3\ 4s/4p$ configurations, not only improves the energies of the the $3p^6\ 3d\ 4s/4p$ levels, but also significantly affects the collision strengths to these levels. We expect that including the $3s^2\ 3p^4\ 3d^3\ 4d/4f$ configurations would also have an appreciable effect on the effective collision strengths for transitions to the 4p/4d/4f levels, but such a calculation is beyond our capability at this time.

For transitions within the ground configuration, we are in very good agreement with the previous R-matrix calculation of Berrington et al. (2000) over a wide temperature range. At high temperatures, our results are in very good agreement with Zeng et al. (2005) for transitions to the 4p, 4f, and $3d^3$ levels. At the lowest published temperature of Zeng et al., where resonance enhancement is starting to play a role, we find larger differences. However, with the exception of transitions to the 4p levels, we are finding that the ratio between the results of Zeng et al. and the present results increases despite our inclusion of resonant

enhancement. The presence of resonances in the present calculation is indicated by the greater variability of the ratio at low temperatures. However, we are unable to explain the larger difference in the background collision strength other than that it follows the trend, also observed by Zeng et al., that larger CI leads to smaller collision strengths for these transitions. Despite this, the agreement is still within 40%. At these low temperatures, the present results serve to provide effective collision strengths where resonant enhancement is important.

Acknowledgements. This work has been funded by PPARC grant PPA/G/S2003/00055. Computational resources were funded by an EPSRC JREI award. M.C.W. would like to thank Jiaolong Zeng for making his data available.

References

Badnell, N. R. 1986, J. Phys. B: At. Mol. Phys., 19, 3827
Badnell, N. R., & Griffin, D. C. 2001, J. Phys. B: At. Mol. Opt. Phys., 34, 681
Berrington, K. A., Nakazaki, S., & Norrington, P. H. 2000, A&AS, 142, 313
Burgess, A. 1974, J. Phys. B: At. Mol. Phys., 7, L364
Burke, P. G., & Berrington, K. A. 1993, Atomic and Molecular Processes: An R-matrix Approach (Bristol: Institute of Physics Publishing)
Griffin, D. C., Badnell, N. R., & Pindzola, M. S. 1998, J. Phys. B: At. Mol. Opt. Phys., 31, 3713
Gu, M. F. 2003, ApJ, 582, 1241
Hummer, D. G., Berrington, K. A., Eissner, W., et al. 1993, A&A, 279, 298
Nussbaumer, H., & Osterbrock, D. E. 1970, ApJ, 161, 811
Nussbaumer, H., & Storey, P. J. 1982, A&A, 113, 21
Quinet, P., & Hansen, J. E. 1996, J. Phys. B: At. Mol. Opt. Phys., 29, 1879
Ralchenko, Yu., Jou, F.-C., Kelleher, D. E., et al. 2007, NIST Atomic Spectra Database, version 3.1.3), http://physics.nist.gov/asd3, September 27
Warner, B., & Kirkpatrick, R. C. 1969, MNRAS, 144, 397
Whiteford, A. D., Badnell, N. R., Ballance, C. P., et al. 2001, J. Phys. B: At. Mol. Phys., 34, 3179
Wigner, E. P., & Eisenbud, L. 1947, Phys. Rev., 72, 29
Witthoeft, M. C., Del Zanna, G., & Badnell, N. R. 2007, A&A, 466, 763
Zeng, J., Liang, G. Y., Zhao, G., & Shi, J. R. 2005, MNRAS, 357, 440